# CHAPTER 4

## ANTISENSE OLIGONUCLEOTIDE-MEDIATED KNOCKDOWN OF TGF-β TYPE I RECEPTORS REDUCES FIBROSIS IN A DUCHENNE MUSCULAR DYSTROPHY MOUSE MODEL

Kemaladewi, D.U., Van Heiningen, S.H., Tran, H.D., Martinez-Garcia, E., Van Ommen, G.J.B., Ten Dijke, P., Aartsma-Rus, A., 't Hoen, P.A.C., Hoogaars, W.M.H.

Submitted.

## ABSTRACT

Duchenne muscular dystrophy (DMD) is caused by lack of functional dystrophin and consequent compromised myofiber integrity. Impaired muscle regeneration and fibrosis are important secondary mechanisms. While antisense oligonucleotides (AONs) have been successfully used to target the primary genetic defect, such approach may be less effective when myofibers are replaced by fibrotic tissue. We present a new AON-mediated strategy to target the secondary pathology through interference with myostatin/TGF-β type I receptors *Acvr1b* (ALK4) and *Tgfbr1* (ALK5) expression. AON-induced exon skipping in the *Acvr1b* and *Tgfbr1* transcripts resulted in functional inhibition of myostatin and/or TGF-β signaling, enhanced myoblast differentiation and delayed fibroblast differentiation. AON treatment of dystrophic *mdx* mice led to significant decreases in the expression of *Acvr1b, Tgfbr1* and fibrosis markers, while inducing regeneration markers. The most prominent effect was achieved in animals treated with a combination of *Acvr1b* and *Tgfbr1* AONs, which markedly reduced fibrosis in diaphragm muscles. Finally, we show that a cocktail of AONs targeting primary and secondary disease mechanisms may hold promise as DMD therapy.

# INTRODUCTION

Duchenne muscular dystrophy (DMD) is a lethal and common form of muscular dystrophy affecting 1 in 3600-6000 newborn boys (Bushby *et al.*, 2010;Emery, 2002). It is caused by nonsense mutations in the *DMD* gene that encodes the structural muscle protein dystrophin. Muscle fibers that lack functional dystrophin have disturbed calcium homeostasis and are more prone to contraction-induced damage, causing severe and progressive muscle degeneration. The persistent damage induces chronic inflammation and elevates the level of multiple cytokines that enhance fibrosis and inhibit muscle regeneration (Serrano *et al.*, 2011).

The DMD therapy currently most advanced in clinical trials employs antisense oligonucleotides (AON), which interfere with the splicing process and reframe the *DMD* transcript, allowing synthesis of internally deleted, partially functional dystrophin (Spitali and Aartsma-Rus, 2012)·(Cirak *et al.*, 2011;Goemans *et al.*, 2011). Since dystrophin is produced by muscle fibers and not by fibroblasts and adipocytes that gradually replace the muscle fibers, the efficacy of the therapy is anticipated to depend on the condition of the level of fibrosis and fatty tissue infiltration. Indeed, in an earlier trial with intramuscular injections of AONs, patients with better muscle quality produced higher amount of dystrophin (van Deutekom *et al.*, 2007). Therefore, a combinatorial approach that simultaneously restores dystrophin and improves the muscle condition may be required.

Members of the Transforming Growth Factor (TGF)-β family of secreted proteins are important determinants of DMD pathology. TGF-β is induced and secreted by immune cells in the inflamed dystrophic muscles in *mdx* mice (Vetrone *et al.*, 2009;Vidal *et al.*, 2008). Furthermore, upregulation of TGF-β is observed in DMD-derived myoblasts and fibroblasts and the expression levels are correlated with severity in the dystrophic mice (Zhou *et al.*, 2006) and the level of fibrosis in DMD patients muscle biopsies (Bernasconi *et al.*, 1995). In addition, skeletal muscle fibers and muscle resident cells including myoblasts, fibroblasts and myofibroblasts secrete the TGF-β family member myostatin, which may further enhance the fibrotic process (Hittel *et al.*, 2009;Li *et al.*, 2008). Myostatin is best known as a potent inhibitor of muscle growth and is specifically expressed in skeletal muscle. Spontaneous mutations or genetic knockdown result in hypertrophic phenotypes and/or improved muscle regeneration (recently reviewed in (Kemaladewi *et al.*, 2012)). Furthermore, another TGF-β family member, activin A, is also involved in regulation of muscle mass (Lee *et al.*, 2010).

TGF-β family members act via activation of signal transduction cascades involving type I and type II transmembrane serine/threonine kinase receptors. TGF-β initiates signaling by binding to TGFBR2, which complexes with the type I receptor TGFBR1 (also known as ALK5). Myostatin uses ACVR2A/B type II receptors and ACVR1B (also known as ALK4) and TGFBR1 type I receptors. Similar to myostatin, activin mainly uses ACVR2A/B and ACVR1B. Their signaling pathways converge towards the phosphorylation of intracellular receptor-regulated SMAD2 and SMAD3 proteins, followed by the association with Co-SMAD (SMAD4) and their translocation into the nucleus (**Fig. 1a**), where it regulates the transcription of a multitude of target genes including genes involved in myogenesis and fibrosis (Heldin *et al.*, 1997).

Similar to their ligands, some of the receptors, including TGFBR2 and TGFBR1 are elevated in DMD animal models and muscle biopsies (Chen *et al.*, 2005;Zhou *et al.*, 2006). This suggests the importance of TGF-β family members in DMD pathology, which makes these signaling cascades attractive targets for DMD therapy. Until recently, most strategies focused on inhibition of the

activity of a single ligand, such as myostatin propeptides (Bogdanovich *et al.*, 2002;Whittemore *et al.*, 2003), antisense oligonucleotides (Kang *et al.*, 2011;Kemaladewi *et al.*, 2011b) or neutralizing antibodies (Wagner *et al.*, 2002), which led to decrease of myostatin expression or inhibition of its ability to induce signaling, as shown by increased muscle size and/or strength and histological improvement.

Myostatin neutralizing antibodies have been shown to be well-tolerated by muscular dystrophy patients in a clinical trial, but did not elicit a significant beneficial response in the muscle, although preclinical studies in the *mdx* mice showed improved muscle mass and functions (Bogdanovich *et al.*, 2002;Krivickas *et al.*, 2009;Wagner *et al.*, 2008). Several promising *in vivo* studies in *mdx* mice with TGF-β antagonists, such as TGF-β neutralizing antibodies (Andreetta *et al.*, 2006;Nelson *et al.*, 2011) or losartan, which reduces TGF-β signaling by inhibiting angiotensin II type I receptor (Cohn *et al.*, 2007;Spurney *et al.*, 2011), led to reduced fibrosis and enhanced muscle regeneration, although the results vary within different dosing regimens and treatment duration. Other strategies target a number of TGF-β ligands, including bone morphogenetic protein (BMP), myostatin, activin A, -B and -AB (Souza *et al.*, 2008) via administration of a soluble form of the type II receptor ACVR2B ligand binding domain (ActRIIB-Fc). A phase II trial in DMD patients showed significant improvement of muscle mass and function, but side effects (nose/gum bleeding) led to termination of the study (clinicaltrials.gov; NCT01099761).

In this study, we adopted the AON-mediated exon skipping strategy to interfere with the TGF-β and myostatin/activin signaling pathways by specifically targeting the type I receptors ACVR1B and TGFBR1. This approach allowed us to dissect the specific and converging effects of ACVR1B and TGFBR1-mediated signaling cascades on DMD pathology as well as to determine the therapeutic potential of these AONs in *mdx* mice.

# RESULTS

## AON-mediated exon skipping in *Acvr1b* and *Tgfbr1*

We developed a strategy to selectively inhibit the function of type I receptors ACVR1B and TGFBR1 in myostatin/activin and/or TGF-β signaling based on AON-mediated exon skipping (**Figs. 1a,b**). Exon 2 of these receptors encodes the ligand binding domain, which is, together with the type II receptor, essential to initiate signaling. Exclusion of exon 2 retains the reading frame, but results in protein that lacks the ligand binding domain **(Fig. 1b)**. Exon 6 encodes part of the kinase domain and targeting this exon will generate an out-of-frame transcript and reduce the production of functional protein **(Fig. 1b)**.

Several AONs with phosphorothioate backbones and 2'-*O*-methyl ribose modifications targeting exon 2 or 6 of *Acvr1b* and *Tgfbr1* were screened in C2C12 mouse myoblast cells for their capacity to induce exon skipping (**Table 1**). RT-PCR analysis showed that exon 2 and exon 6 of *Acvr1b* and *Tgfbr1*, and exon 2 of *Tgfbr1* could successfully be targeted. Sequence analysis confirmed the successful skipping for each exon (Figure S1). The AON targeting *Tgfbr1* exon 6 was later found to be ineffective *in vivo* and therefore omitted from this study. The most effective AONs targeting *Acvr1b* exon 6 and *Tgfbr1* exon 2 were selected for further experiments and will be addressed as A3 and T1, respectively, in the remainder of this manuscript. The target specificity and dose-dependent increase in exon skipping levels for these AONs are shown in **Fig. 1c**.

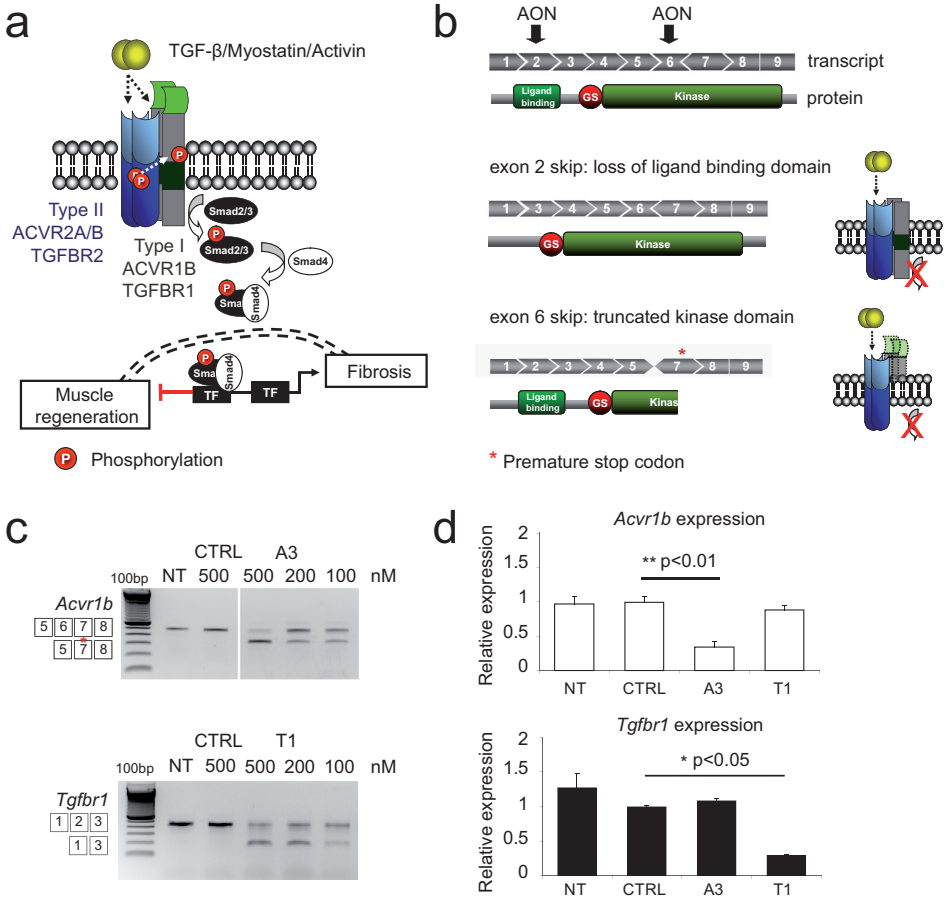


**Figure 1. Schematic overview and *in vitro* proof of principle of *Acvr1b/Tgfbr1*exon skipping.** TGF-β, myostatin and activin bind to type II and type I receptors to activate the Smad2/3-dependent signaling pathways (**a**). The *Acvr1b* and *Tgfbr1* genes consist of nine exons, encoding ligand binding-, Glycine/Serine (GS)-rich and kinase domains (**b**). Each exon is depicted as matching shapes representing the open reading frame and relative to the domains. AON-mediated targeting of exon 2 will result in transcripts that lack the sequence encoding the ligand binding domain and will be translated as proteins without this domain. AON-mediated targeting of exon 6 will disrupt the open reading frame (depicted as unfitted hexagons) and generates a premature stop codon (red asterisk, *) in the resulting transcripts, which leads to premature truncation of protein translation and non functional proteins. AONs targeting exon 6 of *Acvr1b* (A3) or exon 2 of *Tgfbr1* (T1) were transfected at different concentrations into C2C12 mouse myoblasts. Two days after transfection, the efficacy to induce exon skipping was assessed by RT-PCR using *Acvr1b* or *Tgfbr1* specific primers in flanking exons (**c**). Non-transfected (NT) cells or cells transfected with control AON (CTRL, not targeting any mouse mRNA) served as controls. Quantitative real-time PCR was performed to compare *Acvr1b* (**d**, upper panel) or *Tgfbr1* (**d**, lower panel) transcript expression in the 200 nM AON-transfected samples. The data were plotted as averages of at least 3 independent experiments and relative to control. Error bars represent standard deviations. *p<0.05, **p<0.01

We quantified the levels of the full-length transcripts by quantitative RT-PCR (qPCR). As shown in **Fig. 1d**, *Acvr1b* or *Tgfbr1* mRNA expression levels were decreased ~4-fold upon transfection with A3 or T1 AONs, respectively. We also evaluated exon skipping levels in other murine-derived cells expressing *Acvr1b* or *Tgfbr1*, such as mesenchymal stem cells (C3H10 T1/2), endothelial cells, primary and immortalized fibroblasts, and observed comparable exon skipping and knockdown levels (not shown). Importantly, these experiments showed that the AONs specifically reduced the expression of either *Acvr1b* or *Tgfbr1* without affecting the expression of the other receptor.

## Exon skipping in *Acvr1b* and/or *Tgfbr1* abrogates myostatin/TGF-β signaling *in vitro*

We next determined whether *Acvr1b/Tgfbr1* exon skipping interfered with myostatin or TGF-β signaling *in vitro*. We transfected the AONs together with a $(CAGA)_{12}$-luciferase transcriptional reporter construct, which drives expression of a luciferase reporter gene in a Smad3-dependent manner (Dennler *et al.*, 1998). In C2C12 cells, we observed ~9-fold reduction of myostatin-induced luciferase activity upon transfection with A3 AONs, whereas T1 AONs did not alter the responsiveness to myostatin (**Fig. 2a**). In contrast, T1 AONs, but not A3 AONs, decreased myostatin-induced signaling ~4-fold in C3H10 T1/2 cells and other non-myoblast cells tested (**Fig. 2b** and not shown). This is consistent with our recent finding of cell-type specific utilization of the type I receptor for myostatin signaling using siRNA-mediated knockdown of *Acvr1b* or *Tgfbr1* (Kemaladewi *et al.*, 2011a). In addition, the T1 AONs, but not the A3 AONs abrogated TGF-β signaling in both myoblast and non-myoblast cells, showing the specific effect of AON-mediated knockdown of *Tgfbr1* on TGF-β signaling (**Figs. 2c,d**).

## AON-mediated *Acvr1b* and *Tgfbr1* knockdown enhance myoblast and delay fibroblast differentiation

After showing that the AONs exhibited a strong potency in abrogating myostatin or TGF-β signaling, we investigated their effect on myoblast and fibroblast differentiation. We induced C2C12 myoblast differentiation by replacing the proliferation medium with low serum differentiation medium. Twenty four hours after the switch to differentiation medium, cells were transfected with 200 nM A3 or T1 AONs and the differentiation was monitored for up to 7 days. An increase in myotube formation was observed for both A3 and T1 AON-transfected cells, as measured by immunofluorescent staining of desmin and myosin heavy chain and quantification of the differentiation and fusion indices (**Fig. 3a**).

We transfected the AONs into primary fibroblasts isolated from the gastrocnemius muscle of wild-type mice and isolated protein lysates at different time points to measure the expression of classical fibroblast markers such as α-smooth muscle actin (ACTA2), fibronectin and vimentin (**Fig. 3b**). We observed a decrease in ACTA2 protein level 3 days after transfection with A3 or T1 AONs, but these effects were lost at day 5, suggesting that differentiation was delayed but not inhibited. Fibronectin and vimentin expression levels remained unchanged.

Together, these experiments demonstrate that *Acvr1b/Tgfbr1* exon skipping affects several biological activities related to myostatin/TGF-β signaling such as myoblast and fibroblast differentiation.

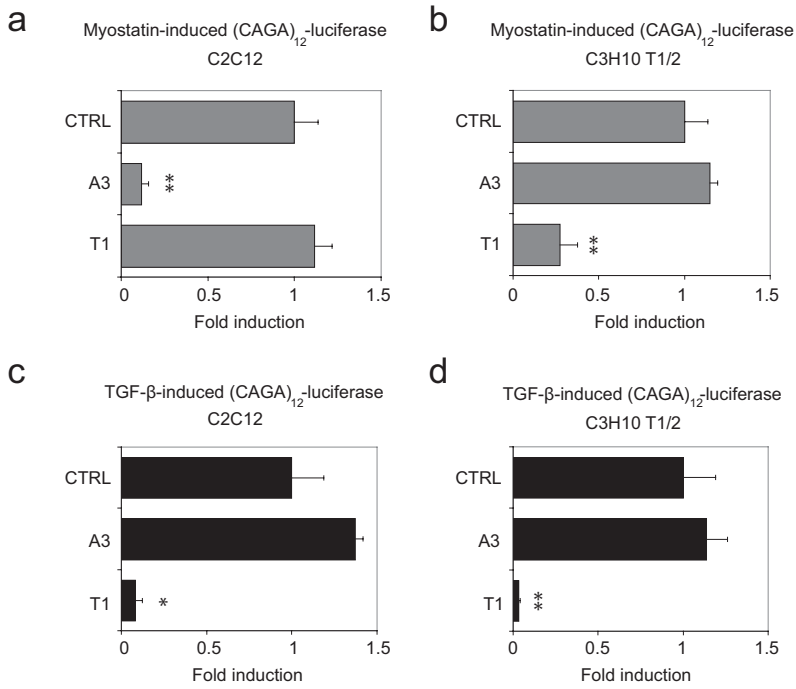


**Figure 2. AON-mediated exon skipping of *Acvr1b* or *Tgfbr1* inhibit myostatin and TGF-β signaling.** Mouse myoblasts C2C12 (**a, c**) and mesenchymal stem cells C3H10 T1/2 (**b, d**) were transfected with $(CAGA)_{12}$-luciferase and CMV-renilla luciferase constructs and either 200 nM of CTRL, A3 or T1 AONs. Following overnight serum starvation, the cells were stimulated with 500 ng/ml of myostatin, 1 ng/ml of TGF-β or minimal medium for 8 hours. Firefly luciferase signals were measured and corrected for renilla signals. The experiments were performed at least three times and each experiment was performed in triplicate. The values were averaged and plotted as fold induction relative to the non stimulated cells, with values for control cells set to 1. Error bars represent standard deviations. *p<0.05, ** p<0.01

## Short-term, intramuscular administration in mdx mice

Following the encouraging results *in vitro*, we proceeded to investigate the effect of *Acvr1b/Tgfbr1* exon skipping in *mdx* mice after intramuscular injection. The A3 or T1 AONs were tested in combination with an AON targeting exon 23 in *Dmd* gene (denoted as DMD AON from now on). This combination was chosen to obtain proof-of-principle for the combination therapy and to have a positive control for the *in vivo* administration procedure. We injected one of the triceps muscles of 5-weeks old *mdx* mice for 4 consecutive days with a mixture of A3 or T1 and DMD AONs. The contralateral muscle received a cocktail of control scrambled A3 or T1 (designated as AScr or TScr, respectively) and DMD AONs. The animals were sacrificed 10 days after the final injection.

As shown in **Fig. 4a**, *Acvr1b* exon skipping was observed in all muscles injected with the A3 AON but not in the contralateral control muscles injected with AScr AON. Similarly, the muscles injected with T1 AON demonstrated *Tgfbr1* exon 2 skipping, whereas the control muscles did not. Importantly, these AONs did not interfere with the DMD AON, resulting in simultaneous exon skipping in both genes. Further quantification of the remaining transcripts by qPCR resulted in a significant knockdown

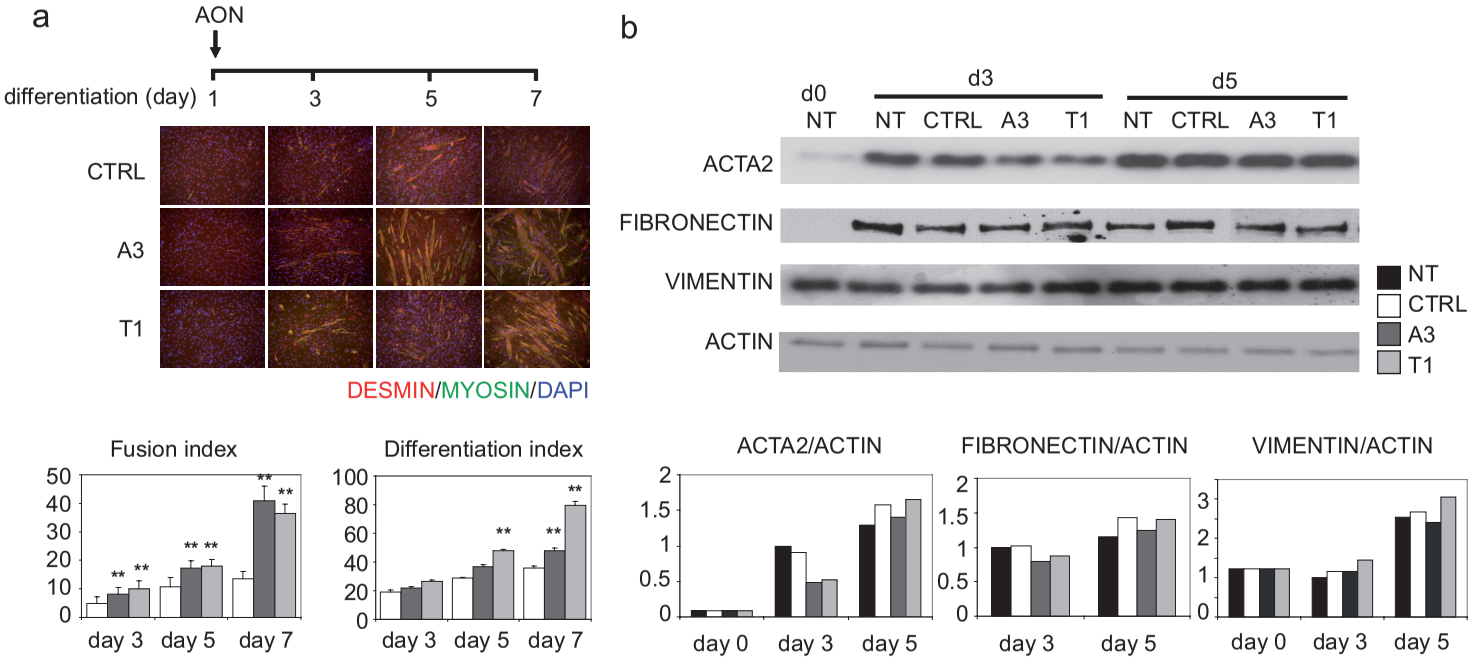


**Figure 3. AON-mediated exon skipping in *Acvr1b* and *Tgfbr1* enhance myoblast differentiation and delay fibroblast differentiation.** C2C12 myoblasts were grown to ~80% confluency and differentiation was induced by switching the medium to low serum. After 1 day of differentiation, cells were transfected with 200 nM of CTRL, A3 or T1 AONs and allowed to further differentiate. Immunofluorescent staining for desmin (red), myosin (green) and DAPI (blue) was performed at the indicated time points to assess the myogenic differentiation (**a**). Fusion and differentiation indexes were calculated as described in material and methods. Error bars represent standard deviations. **p<0.01. Primary fibroblasts isolated from gastrocnemius muscles of wild type mice were grown to ~60-70% confluency (d0) and transfected with 200 nM of CTRL, A3 or T1 AONs. Proteins were isolated at the indicated time points and analyzed for the expression of α-smooth muscle actin (ACTA2), fibronectin and vimentin by western blot and quantified densitometrically using actin as loading controls (**b**).

of 80% and 50% of full-length *Acvr1b* and *Tgfbr1* transcripts in the muscles injected with A3 and T1 AON, respectively (**Fig. 4b**). Target specificity of these AONs was maintained *in vivo*, because the A3 AON did not alter the expression of full length *Tgfbr1* and vice versa.

To further assess whether there was any effect on muscle regeneration or fibrosis, several target genes that regulate muscle differentiation/regeneration (*Myog*) or that are involved in fibrosis (*Col1a1, Serpine1, Ctgf*) were measured by qPCR (**Fig. 4c**). The expression of *Myog* was significantly increased ~2 fold in the muscles injected with the A3 AON. A similar trend was observed upon T1 AON injection, but the increase was not statistically significant. *Col1a1* expression level decreased ~2 and 4 fold upon *Acvr1b* and *Tgfbr1* knockdown, respectively. Decreases of *Serpine1* (also known as *Pai1*) and *Ctgf,* two other genes correlated with fibrosis, were also observed upon *Tgfbr1* knockdown. Interestingly, these genes were upregulated upon *Acvr1b* knockdown. These opposite changes in *Serpine1* gene expression upon *Acvr1b* and *Tgfbr1* knockdown were confirmed by western blot analysis and are indicative for the different roles of *Acvr1b* and *Tgfbr1* in the disease pathology (**Fig. 4d**). Although there was considerable variation, SMAD2 phosphorylation levels in these muscles were generally reduced, suggesting an overall reduction in myostatin/activin/TGF-β signaling upon A3 or T1 AON administration (**Fig. 4d**).

## Systemic AON administration in *mdx* mice

We next investigated whether a longer-term, systemic downregulation of *Acvr1b* and *Tgfbr1* would also be feasible and beneficial. Based on the sequences of the existing A3 and T1 AONs with 2'-O-methyl phosphorothioate modifications, we designed the morpholino counterparts with octa-guanidine conjugates (Vivo Morpholino, further denoted as VM), because this chemistry has been described to enhance tissue uptake upon systemic administration (Wu *et al.*, 2009). Direct comparison of both chemistries after intramuscular injections indeed showed that the VM led to higher exon skipping efficiencies in most tissues isolated (Figure S2).

*Mdx* mice were treated intravenously with 6 mg/kg VM targeting either *Acvr1b* (VM-A3) or *Tgfbr1* (VM-T1) once weekly for 6 weeks. Additional groups received either a cocktail of VM-A3 and VM-T1 or PBS as a control. The animals were sacrificed 10 days after the last injection and the triceps and diaphragm muscles were harvested. RT-PCR analysis of the triceps showed prominent *Acvr1b* exon skipping in the animals treated with either the VM-A3 AON or a combination of VM-A3 and VM-T1 AONs (**Fig. 5a**). Similarly, *Tgfbr1* exon skipping was observed in the VM-T1 AON treated mice as well as in the combination AON groups. Subsequent quantification using qPCR showed 30-40% knockdown of full-length *Acvr1b* and 20-30% knockdown of full-length *Tgfbr1* relative to the PBS-injected mice (**Fig. 5b**). The expression of *Myog* mRNA increased in the AON-treated animals, but significance was only obtained in the group treated with the combination of VM-A3 and VM-T1 (**Fig. 5c**). The mRNA expression of the fibrotic marker *Acta2* decreased in all groups, and the protein level decreased significantly in the group treated with the combination of AONs (**Figs. 5c,d**). In contrast, the fibrotic marker *Col1a* remained unchanged. Decrease of SMAD2 phosphorylation levels in the triceps was only observed in the VM-T1 AON- and combination AON groups, while the level in the VM-A3 AON-treated triceps remained similar to control samples (**Fig. 5d**). This was accompanied by lower SERPINE1 protein levels in all AON-treated groups, although a significant decrease was only observed in the VM-A3 AON-treated mice. Muscle fiber size was analyzed to determine if treatment with these AONs resulted in muscle fiber hypertrophy as was described for several myostatin inhibitors (Dumonceaux *et al.*, 2010;Kang *et al.*, 2011). We did not observe any significant differences in fiber size, although

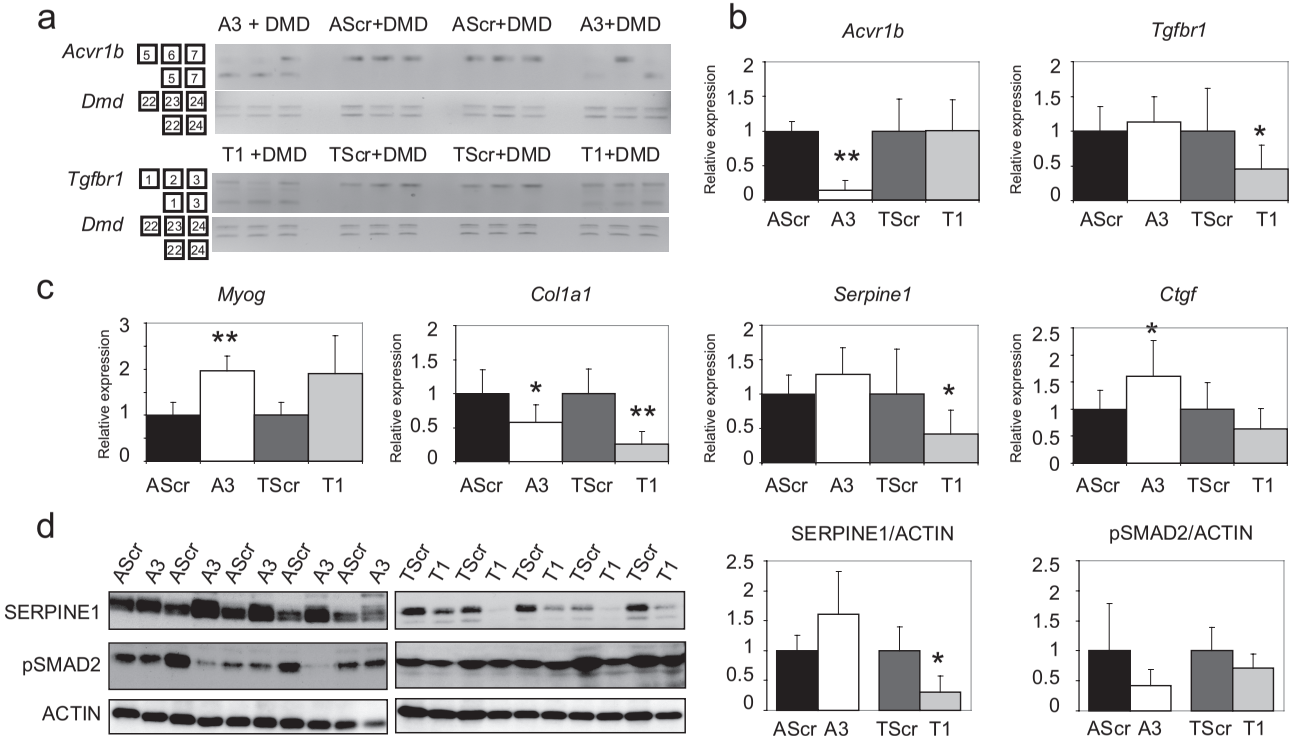


**Figure 4. Effect of *Acvr1b/Tgfbr1*exon skipping after intramuscular injections in *mdx* mice.** The triceps of *mdx* mice (n=6 *mdx*/group) were injected with combinations of A3 and DMD AONs, whereas the contralateral triceps received a combination of DMD and AScr (the scrambled control for A3) AONs. Another group of *mdx* mice received a combination of T1 and DMD AONs in the triceps muscles, and similarly, the scrambled T1 (TScr) and DMD AONs were combined and injected in the contralateral muscles as control. All animals were sacrificed 10 days after the last injection. RNA was isolated from each triceps and analyzed by RT-PCR (**a**) and qPCR (**b,c**) for the detection of the exon skipping product and the expression of *Acvr1b, Tgfbr1, Myog, Col1a1, Serpine1* and *Ctgf*. Protein lysates were analyzed for SERPINE1 and phosphorylated SMAD2 by Western blot and quantified densitometrically using ACTIN as loading control (**d**). Error bars in **b, c** and **d** represent standard deviations. Statistical analysis was performed using the Student's t-test. * p<0.05, ** p<0.01

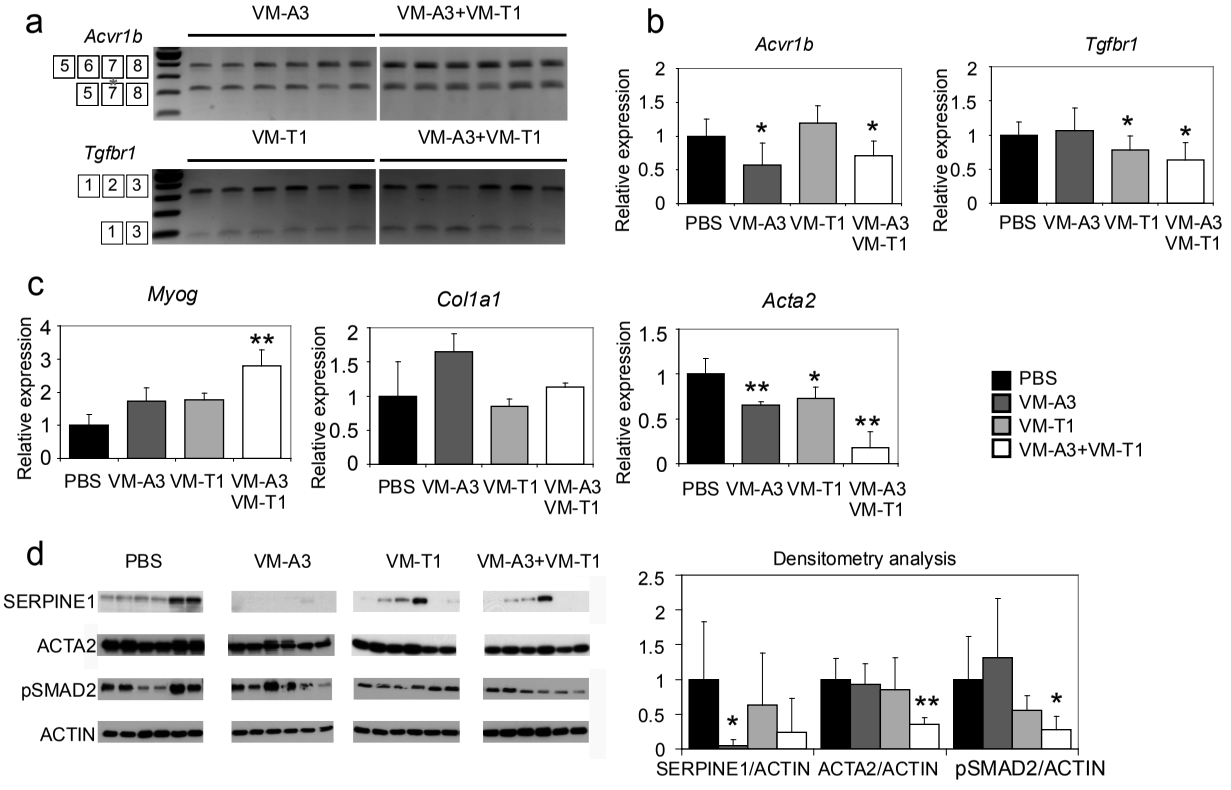


**Figure 5. Effect of AON-mediated exon skipping in the triceps following systemic administration.** *Mdx* mice were intravenously injected with PBS, VM-A3, VM-T1 or a combination of VM-A3+VM-T1 AONs (n=6 per group) weekly for 6 weeks and sacrificed 4 days after the last injection. Triceps were isolated and analysed for detection of exon skip producs by RT-PCR (**a**). qPCR was performed to quantify the expression of *Acvr1b*, *Tgfbr1* (**b**), *Myog*, *Col1a1* and *Acta2* (**c**), corrected to *Gapdh* as a housekeeping gene. Protein lysates were analysed for SERPINE1, ACTA2 and phosphorylated SMAD2 levels by western blot and quantified densitometrically using ACTIN as loading control (**d**). Statistical analysis was performed using the Student's t-test. * p<0.05, ** p<0.01

there was a trend towards presence of bigger fibers in the VM-T1 AON treated triceps compared to the PBS control group (Figure S3).

Next, we analyzed the diaphragms of the treated *mdx* mice, since this muscle is known to show the most pronounced fibrosis in the *mdx* mouse model (Stedman *et al.*, 1991). RT-PCR and qPCR analysis showed prominent exon skipping of *Acvr1b* and *Tgfbr1* (**Fig. 6a**), leading to ~60-70% and 50-60% knockdown of *Acvr1b* and *Tgfbr1* full length transcripts, respectively (**Fig. 6b**). Phosphorylated SMAD2 and SERPINE1 protein levels, and ACTA2 mRNA and protein levels decreased upon treatment with VM-A3 and VM-T1 AONs, which was particularly prominent in the combination treatment group (**Figs. 6c,d**), and supporting the findings in the triceps. In contrast to the results observed in the triceps, *Col1a1* transcripts decreased, whereas *Myog* remained unchanged (**Fig. 6c**). Histological analysis using Sirius red staining as a measure for collagen deposition and fibrosis was performed. VM-A3 AON-treated animals did not show any significant differences in fibrotic area (43.59 ± 10.13 %) compared to the PBS-treated animals (47.11 ± 7.29 %), whereas in the VM-T1 AON- and combination of VM-A3 and VM-T1 AONs-treated groups the fibrotic percentages decreased to 33.38 ± 5.94 % and 29.92 ± 4.90 %, respectively (**Fig. 7**).

Serum was collected at the end of the treatment period. We observed a trend of decrease in serum creatine kinase levels, which is one of the indicators of muscle damage, in AON-treated *mdx* mice towards the wild-type levels in the end of the study (Figure S4). Although the differences of VM-A3, VM-T1 and combination AONs groups compared to control group were not significant due to the high variation between animals, this result suggested a general improvement in the muscle fiber integrity upon treatment, again especially in animals treated with the combination of VM-A3 and VM-T1 AONs. Finally, there was no significant increase in the liver enzymes such as glutamic-pyruvic transaminase (GPT) and glutamic-oxaloacetic transaminase (GOT), whereas the urea level was slightly elevated, although still within an acceptable range (Figure S4). Overall, these blood enzyme parameters indicate that the treatment was well-tolerated by the animals.

## DISCUSSION

The absence of dystrophin in DMD leads to progressive myonecrosis, chronic inflammation and extensive fibrosis. The latter is associated with overactive TGF-β signaling (Bernasconi *et al.*, 1995), which also impedes muscle regeneration (Liu *et al.*, 2001). In this study we present a novel approach to inhibit the signaling activity of myostatin, activin and TGF-β, three signaling proteins that contribute to muscle regeneration and fibrosis, using AON-mediated exon skipping in *Acvr1b* and/or *Tgfbr1* receptors transcripts.

In our previous study, we showed that both myostatin and TGF-β utilize TGFBR1 as the main type I receptor in fibroblasts (Kemaladewi *et al.*, 2011a), and in this study we confirmed that AON-mediated knockdown of *Acvr1b* does not inhibit myostatin signaling in non-myogenic cells *in vitro*. Nonetheless, we observed a delay in fibroblast differentiation and a reduction of the expression of most fibrosis-related genes *in vivo* not only after administration of AONs targeting *Tgfbr1* but also when targeting *Acvr1b*. This suggests that the effects on fibrosis conveyed via *Acvr1b* are not due to an effect on myostatin/TGF-β signaling but due to the modulation of signaling by activin or another member of the TGF-β family. This may also explain why the strongest effects on fibrosis are observed when targeting both *Tgfbr1* and *Acvr1b*.

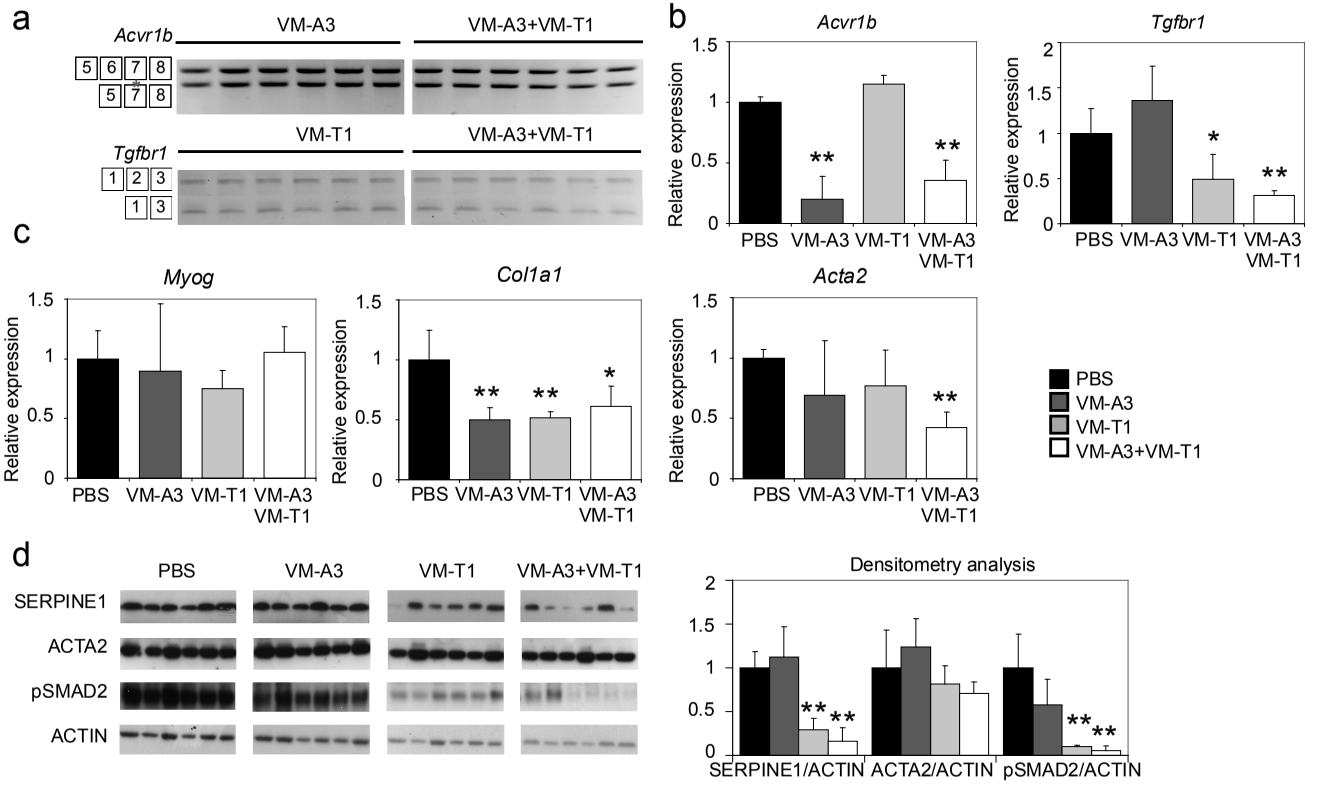


**Figure 6. Effect of AON-mediated exon skipping in the diaphragm following systemic administration.** Diaphragm muscles were isolated from the same experimental setup as described in figure 5 and analysed for exon skipping by RT-PCR (**a**), expression of *Acvr1b, Tgfbr1* (**b**), *Myog, Col1a1* and *Acta2* (**c**), corrected to *Gapdh* expression values by qPCR. Protein lysates were analysed for SERPINE1, ACTA2 and phosphorylated SMAD2 levels by western blot and quantified densitometrically using ACTIN as loading control (**d**). Note that the levels of phosphorylated SMAD2 in diaphragms are generally higher than in triceps. Statistical analysis was performed using the Student's t-test. * p<0.05, ** p<0.01

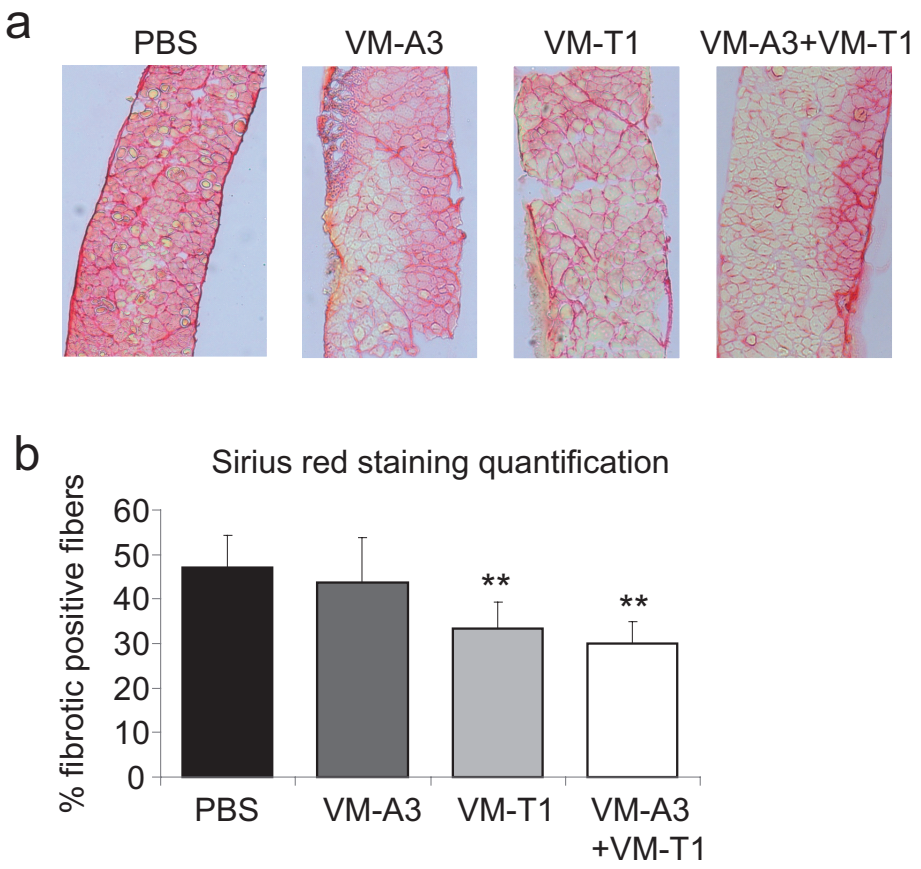


**Figure 7. Sirius Red staining on diaphragm muscles following systemic administration.** Diaphragm cross-sections were stained for connective tissue/collagen deposition by Sirius Red. Representative images are shown for each treatment group (**a**). The red stained area in the fibers was quantified and expressed relative to the total fiber area using ImageJ. 4-5 muscle sections per animal were analysed (**b**). Error bars represent standard deviations for n=6 mice per group. Statistical analysis was performed using Student's t-test. *p<0.05.

The significant reduction of fibrosis observed in diaphragm was not observed in triceps, most likely because of much lower level of fibrosis in the triceps of the *mdx* mice compared to the diaphragm. In contrast, the expression of regeneration marker *Myog* was enhanced in triceps but not in the diaphragm upon treatment with the single AONs and more pronounced with the combination of AONs. This may be explained by the higher degree of fibrosis in the diaphragm, since it has been proposed that repair of fibrotic tissue precedes muscle regeneration (Moyer and Wagner, 2011). Despite the demonstrated stimulatory effects of the AONs on myoblast differentiation and *Myog* expression, we did not observe a clear effect on muscle fiber size or percentage of centrally located nuclei. This may suggest that the level of functional repression of these receptors *in vivo* was not enough to result in muscle hypertrophy, which may be beneficial since hypertrophy is not necessarily linked to increase muscle strength (Amthor *et al.*, 2007).

In this study we also confirmed that dystrophin exon skipping can be combined with other exon skipping strategies, namely *Acvr1b/Tgfbr1* as a cocktail and administered in single injection. Such a combinatorial approach will tackle the primary genetic defect by restoration of dystrophin expression, as well as improve both muscle quality and function. Importantly, the effect of combinatorial approaches that both target myostatin/TGF-β signaling and restore dystrophin expression on DMD pathology has not been investigated extensively. One study reported that a combination of myostatin repression and dystrophin restoration resulted in improved muscle force generation (Dumonceaux *et al.*, 2010). However, this approach was based on intramuscular delivery of an AAV vector. We previously showed that exon skipping of myostatin and *Dmd* is also possible, but in contrast to the systemic efficiency of *Acvr1b* and *Tgfbr1* AONs, the efficiency of myostatin AON was low *in vivo* (Kemaladewi *et al.*, 2011b). Future studies are therefore aimed at determining the systemic additive of synergistic effects of *Acvr1b/Tgfbr1/Dmd* AON cocktails in DMD animal models. From a pharmaceutical formulation perspective, combining multiple AONs of the same chemistry would be superior to combining AONs with other TGF-β inhibitors, such as neutralizing antibody (Bogdanovich *et al.*, 2002), soluble receptors (Pistilli *et al.*, 2011), or small molecule inhibitors (Kano *et al.*, 2009). Moreover, once weekly treatment with AONs would be more favorable compared to other compounds that require more frequent injections and are less stable.

Finally, we did not observe serious adverse events of VM AONs after 6-weeks treatment in *mdx* mice. Although these results are indicative for the safety of the chemical compounds themselves, additional toxicity due to off-target effects in other tissues cannot be excluded. We provided initial assessments of several safety parameters such as liver enzymes and urea, and only urea levels were slightly but not significantly elevated upon treatment and still within normal ranges. Gross pathology examination of the kidney did not reveal consistent alterations in kidney structure (unpublished observation). It is possible, however, that our approach will benefit from muscle-specific targeting strategies.

Alterations in the signaling of TGF-β family members are pleiotropy and have been associated with many diseases, including several tissue-specific fibrotic disorders. In liver fibrosis, activin A expression was elevated and associated with cirrhosis progression (Sugiyama *et al.*, 1998), which could be attenuated using the activin antagonist follistatin (Patella *et al.*, 2006). Similarly, TGF-β induces fibrosis in various adult tissues, including liver, lung and kidney, which leads to the formation of extracellular matrix-producing fibroblasts (Kalluri and Neilson, 2003). Therefore, the benefits of this treatment may extend to other diseases where TGF-β signaling is altered. Moreover, the AONs targeting *Acvr1b* or *Tgfbr1* may be applied in a more specific context by either targeting activin or TGF-β in diseases that show aberrant activation of one or the other signaling cascade.

# MATERIALS AND METHODS

## Cell culture and AON transfections

Mouse myoblasts C2C12 (ATCC) were maintained in Dulbecco's modified Eagle's medium (DMEM) with 10% FBS, 1% glucose and 2% glutamax (Invitrogen) and mesenchymal stem cells C3H10 T1/2 (ATCC) were grown in α-MEM medium with 10% FBS (Invitrogen) at 37°C with 10% and 5% $CO_2$,

respectively. The differentiation medium for C2C12 was DMEM with 2% FBS, 1% glucose and 2% glutamax (Invitrogen). Primary fibroblasts were isolated by mincing the gastrocnemius muscles of wild-type *C57BL/10ScSnJ* mice and grown in Nut-Mix F10 (HAM) medium supplemented with 20% FBS at 37°C, 5% CO2 for ~2 weeks with routine medium changes. The emerging cells were isolated, pre-plated and grown on collagen-coated plates (1:30, Vitrogen). AONs with phosphorothioate backbones and 2'-*O*-methyl ribose modifications were purchased from Eurogentec, Belgium. The sequences are listed in **Table 1**. The transfection was done using Lipofectamine 2000 (Invitrogen) according to the manufacturer's instructions (except in the luciferase and myogenic differentiation assays below).

## Luciferase reporter assay

Cells were seeded at a density of 5000 cells/well on white µclear 96-wells plates (Greiner bio-one) until 70% confluent and transiently transfected with 100 ng of $(CAGA)_{12}$-Luc, 10 ng of pRL-CMV and 200 nM of the indicated AON using Dharmafect Duo (Thermo Scientific). Following an overnight serum starvation, cells were stimulated with 1ng/ml TGF-β (kindly provided by OSI Pharmaceuticals Inc, NY), 500 ng/ml myostatin (R&D Systems) or serum free medium for 8 hours. The cells were lysed using DualGlo Luciferase Assay Kit (Promega) and the luciferase signals were read in the Multilabel Counter (Perkin Elmer). Renilla luciferase signals were used to normalize for the transfection efficiency. Experiments were conducted in triplicates and repeated at least 3 times. Statistical analysis was performed using Student's t-test and p-values <0.05 were considered significant.

**Table 1.** Antisense oligonucleotides (AON) used in this study

| Chemistry-AON | Target gene | Sequences (5'-3') | Efficacy |
|---|---|---|---|
| A1 | *Acvr1b* exon 2 | AUGGAGACCAUGCAAGCCCCA | - |
| A2 | *Acvr1b* exon 2 | UUCCAGCAGGAACCAGCUCCA | - |
| A3 | *Acvr1b* exon 6 | UGGUGUCAGUGACCGCAUCAU | ++ |
| A4 | *Acvr1b* exon 6 | UGACUUCAAGUCUCGAUGAGC | + |
| T1 | *Tgfbr1* exon 2 | GCAGUGGUCCUGAUUGCAGCA | ++ |
| T2 | *Tgfbr1* exon 2 | CUUUGUACAGAGGUGGCAGAA | + |
| T3 | *Tgfbr1* exon 6 | AUCUGUGGCAGAAUCAUGUCU | +/- |
| T4 | *Tgfbr1* exon 6 | UCUGUGGUUUGGAGCAAUAUC | + |
| CTRL | N/A | UUCUCAGGAAUUUGUGUCUUU | N/A |
| AScr | N/A | UAUCUUGACCGCCUGAGAGGG (Scrambled of A3 sequences) | N/A |
| TScr | N/A | AUCUGCGAUCGGGACUUUGCA (Scrambled of T1 sequences) | N/A |
| VM-A3 | *Acvr1b* exon 6 | TCTATGGTGTCAGTGACCGCATCAT | ++ |
| VM-T1 | *Tgfbr1* exon 2 | GCAGTGGTCCTGATTGCAGCAATAT | ++ |
| VM-T3 | *Tgfbr1* exon 6 | TTGTATCTGTGGCAGAATCATGTCT | + |
| DMD | *Dmd* exon 23 | GGCCAAACCUCGGCUUACCU | ++ |

VM denotes Vivo Morpholino, while the rests were 2'-*O*-methyl phosphorothioate modified AONs;
N/A = not targeting any mouse genes;
- = ineffective in the *in vitro* screening and not tested further *in vivo*;
+/- = effective *in vitro* but unable to induce exon skipping *in vivo*;
+ and ++ = efficacy as tested *in vivo*

## Myoblast and fibroblast differentiation assay

Myogenic differentiation assays for C2C12 were performed and quantified as described before (Kemaladewi *et al.*, 2011a). In brief, differentiation index is the percentage of myosin-positive cells of all myogenic cells, whereas fusion index is measured as the average number of nuclei in myosin-positive cells. For the fibroblast differentiation experiment, 60-70% confluent fibroblasts (d0) were transfected with the indicated AON and the medium was switched to DMEM with 2% FBS. Protein lysates were isolated after 3 and 5 days for immunoblotting analysis.

## *In vivo* AON treatments

All animal experiments were performed after the approval of the Animal Experimental Committee of the LUMC (DEC07195). In the intramuscular experiments, the triceps muscles of *mdx* mice (5-6 weeks old, n=6) were injected with a mix of 40 µg each of A3 (Eurogentec) and DMD (kindly provided by Prosensa Therapeutics). The contralateral triceps, serving as controls, were injected with a mix of AScr and DMD at the same dose. Another group of 6 *mdx* mice received a mix of DMD and T1 or TScr AONs. The injection was performed consecutively for 4 days, with a 24 hours interval between the second and third injections. The animals were put under isofluorane while being injected and sacrificed 10 days after the last injection by cervical dislocation. Tissues were isolated, snap frozen in liquid nitrogen-chilled isopentane and stored in -80°C until further use.

For the systemic treatment, the animals received 6 mg/kg VM-A3, VM-T1 or combination of VM-A3+VM-T1 (thus 12 mg/kg) (GeneTools) intravenously via tail vein injections. The sequences are shown in Table 1. Control animals received sterile PBS at the equivalent volume of 100 µl. Each treatment group consisted of 6 *mdx* mice of 5-6 weeks old. The injections were performed once a week for 6 weeks and the animals were sacrificed 4 days after the last injection. Prior to sacrificing, blood samples were taken via the tail tip (see blood enzyme measurement section below). The tissues were harvested as mentioned above.

## RNA isolation, RT-PCR, qPCR

Cells were lysed and RNA was directly isolated using NucleoSpin RNA II kit (Macherey-Nagel) according to the manufacturer's instruction. Tissues were first sectioned, collected in 1.4 mm Zirconium Beads pre-filled tubes (OPS Diagnostics) and homogenized using a MagNA Lyser (Roche Diagnostics) in lysis buffer supplied by the NucleoSpin RNA II kit, followed by RNA isolation. N6-primed cDNA was synthesized from 500 ng RNA using RevertAid H Minus M-Mulv Reverse Transcriptase (MBI Fermentas) according to the manufacturer's instructions. Ten times diluted cDNA was amplified by PCR using AmpliTaq Gold GeneAmp kit (Roche). A nested PCR was performed for dystrophin as previously published (Kemaladewi *et al.*, 2011b). Quantitative PCR was performed in a LightCycler 480 using SensiMix reagents (Bioline). The expression levels were analyzed using the LinReg qPCR method (Ruijter *et al.*, 2009) and normalized to expression values of the housekeeping gene *Gapdh*, which is expressed at similar levels in muscles of wild type and *mdx* mice. Primer sequences and detailed PCR conditions are available upon request. Statistical analysis was performed using the Student's t-test.

## Protein isolation and Western blotting

Protein lysates from the cells were isolated using a previously described method (Kemaladewi *et al.*, 2011b). Sectioned muscles collected in the Zirconium beads tubes were homogenized in 500

µl of RIPA homogenizer buffer (50 mM Tris HCl pH 7.4, 150 nM NaCl, 1 mM EDTA supplemented with Phosphatase and Protease inhibitor cocktails (Roche)) and lysed with a MagNA Lyser. Following 2 sonification steps, 500 µl of RIPA double detergents buffer (2% deoxycholate, 2% NP40 and 2% Triton X-100 in RIPA homogenizer buffer) was added to the lysates, which were then incubated for 45 minutes at 4°C with rotation and centrifuged for 10 minutes at 30000g. The protein concentration of the supernatant was measured using the BCA assay. SDS page and western blotting were performed using standard protocols. The primary antibodies used were rabbit polyclonal anti-C-terminally phosphorylated Smad2 (Ludwig Institute for Cancer Research, Uppsala, Sweden, 1:10000), PAI1/SERPINE1 (Santa Cruz, 1:1000), vimentin (Cell Signaling, 1:1000) and mouse monoclonal anti α-smooth muscle actin (Sigma-Aldrich, 1:10000), fibronectin (Santa Cruz, 1:5000). Goat anti-rabbit and goat anti-mouse IgG HRP (Santa Cruz) were used at 1:5000 dilution. The detection was performed using SuperSignal West Pico or West Femto Chemiluminescent (Thermo Scientific) and densitometry analysis was performed using ImageJ software (NIH). Statistical analysis was performed using the Student's t-test.

## Blood enzyme measurement

Blood samples were collected in 0.8 ml Lithium Heparin tubes (Greiner bio-one) from a cut in the tail. Plasma was isolated after 5 minutes centrifugation at 30000g at 4°C and diluted 10 times for the measurements of Creatine Kinase, GOT and GPT levels, or undiluted for urea levels using Reflotron test strips in the Reflotron plus machine (Roche).

## Histology and morphometric analysis

Muscle cryo-sections of 8 µm were stained with Hematoxylin/Eosin and the average fiber size from a total of 300 fibers were measured and semi-automatically quantified by measuring the minimum Feret's diameter based on the previously published methods (van Putten *et al.*, 2010). Sirius red staining was carried out on cold aceton-fixed sections, which were subsequently dried at room temperature and washed in demineralised water. The sections were incubated in 0.2% phosphomolybdic acid for 5 minutes and directly immersed in 0.1% Sirius red reagents for another 5 minutes. Excess staining solutions were removed by soaking the slides in demineralised water and blotting them dry with paper towel. Muscle sections were immediately dehydrated in 70%, 80%, 90% and 100% ethanol (1 minute for each wash) and cleared in xylene prior to embedding in Pertex (Histolab). Images were taken using Pannoramic MIDI 1.14 scanner, imported with 3D Histech software (3DHISTECH Ltd.) and analysed using colour deconvolution plugin of the ImageJ software. The scoring was performed independently by two blinded-investigators.

# ACKNOWLEDGMENTS

We appreciate the excellent technical help and valuable input from Christa Tanganyika-de Winter, Ingrid Verhaart, Wouter Leonhard, Daniela Salvatori, David de Gorter, Frans Prins, Dorien Peters and Johan den Dunnen (LUMC). We are grateful to Prosensa Therapeutics B.V. for providing the DMD AONs. We also wish to thank Mark Einerhand at Vereenigde BV for the help with technology transfer and critical reading of the manuscript. Some of the authors are co-inventors on several patent applications for antisense sequences, exon skipping

technologies and therapeutic approach based on modulation of TGF-β and BMP expression. The Dutch Duchenne Parent Project, Center for Biomedical Genetics, Netherlands Institute for Regenerative Medicine and Netherlands Organization for Scientific Research (NWO) are gratefully acknowledged for financially supporting this study.

## AUTHOR CONTRIBUTIONS

DUK, PtD, AAR, PACtH, WMH devised the concept, study and experimental designs. DUK, SHvH, HDT, EMG, WMH performed experiments. DUK, AAR, PACtH, WMH analysed and interpreted the data. DUK wrote the manuscript. All authors read and agreed on the manuscript.

## REFERENCE LIST

1. Bushby, K, Finkel, R, Birnkrant, DJ, Case, LE, Clemens, PR, Cripe, L (2010). Diagnosis and management of Duchenne muscular dystrophy, part 1: diagnosis, and pharmacological and psychosocial management. *Lancet Neurol* **9**: 77-93.
2. Emery, AE (2002). The muscular dystrophies. *Lancet* **359**: 687-695.
3. Serrano, AL, Mann, CJ, Vidal, B, Ardite, E, Perdiguero, E, Munoz-Canoves, P (2011). Cellular and molecular mechanisms regulating fibrosis in skeletal muscle repair and disease. *Curr Top Dev Biol* **96**: 167-201.
4. Spitali, P and Aartsma-Rus, A (2012). Splice modulating therapies for human disease. *Cell* **148**: 1085-1088.
5. Cirak, S, rechavala-Gomeza, V, Guglieri, M, Feng, L, Torelli, S, Anthony, K *et al*. (2011). Exon skipping and dystrophin restoration in patients with Duchenne muscular dystrophy after systemic phosphorodiamidate morpholino oligomer treatment: an open-label, phase 2, dose-escalation study. *Lancet* **378**: 595-605.
6. Goemans, NM, Tulinius, M, van den Akker, JT, Burm, BE, Ekhart, PF, Heuvelmans, N *et al*. (2011). Systemic administration of PRO051 in Duchenne's muscular dystrophy. *N Engl J Med* **364**: 1513-1522.
7. van Deutekom, JC, Janson, AA, Ginjaar, IB, Frankhuizen, WS, artsma-Rus, A, Bremmer-Bout, M (2007). Local dystrophin restoration with antisense oligonucleotide PRO051. *N Engl J Med* **357**: 2677-2686.
8. Vetrone, SA, Montecino-Rodriguez, E, Kudryashova, E, Kramerova, I, Hoffman, EP, Liu, SD *et al*. (2009). Osteopontin promotes fibrosis in dystrophic mouse muscle by modulating immune cell subsets and intramuscular TGF-beta. *J Clin Invest* **119**: 1583-1594.
9. Vidal, B, Serrano, AL, Tjwa, M, Suelves, M, Ardite, E, De, MR *et al*. (2008). Fibrinogen drives dystrophic muscle fibrosis via a TGFbeta/alternative macrophage activation pathway. *Genes Dev* **22**: 1747-1752.
10. Zhou, L, Porter, JD, Cheng, G, Gong, B, Hatala, DA, Merriam, AP *et al*. (2006). Temporal and spatial mRNA expression patterns of TGF-beta1, 2, 3 and TbetaRI, II, III in skeletal muscles of mdx mice. *Neuromuscul Disord* **16**: 32-38.
11. Bernasconi, P, Torchiana, E, Confalonieri, P, Brugnoni, R, Barresi, R, Mora, M *et al*. (1995). Expression of transforming growth factor-beta 1 in dystrophic patient muscles correlates with fibrosis. Pathogenetic role of a fibrogenic cytokine. *J Clin Invest* **96**: 1137-1144.
12. Hittel, DS, Berggren, JR, Shearer, J, Boyle, K, Houmard, JA (2009). Increased secretion and expression of myostatin in skeletal muscle from extremely obese women. *Diabetes* **58**: 30-38.
13. Li, ZB, Kollias, HD, Wagner, KR (2008). Myostatin directly regulates skeletal muscle fibrosis. *J Biol Chem* **283**: 19371-19378.
14. Kemaladewi, DU, 't Hoen, PA, ten Dijke, P, van Ommen, GJ, Hoogaars, WM (2012). TGF-β signaling in Duchenne muscular dystrophy. *Future Neurology* **7**: 209-224.
15. Lee, SJ, Lee, YS, Zimmers, TA, Soleimani, A, Matzuk, MM, Tsuchida, K *et al*. (2010). Regulation of muscle mass by follistatin and activins. *Mol Endocrinol* **24**: 1998-2008.
16. Heldin, CH, Miyazono, K, ten Dijke, P (1997). TGF-beta signalling from cell membrane to nucleus through SMAD proteins. *Nature* **390**: 465-471.
17. Chen, YW, Nagaraju, K, Bakay, M, McIntyre, O, Rawat, R, Shi, R *et al*. (2005). Early onset of inflammation and later involvement of TGFbeta in Duchenne muscular dystrophy. *Neurology* **65**: 826-834.
18. Bogdanovich, S, Krag, TO, Barton, ER, Morris, LD, Whittemore, LA, Ahima, RS *et al*. (2002). Functional improvement of dystrophic muscle by myostatin blockade. *Nature* **420**: 418-421.

19. Whittemore, LA, Song, K, Li, X, Aghajanian, J, Davies, M, Girgenrath, S *et al*. (2003). Inhibition of myostatin in adult mice increases skeletal muscle mass and strength. *Biochem Biophys Res Commun* **300**: 965-971.
20. Kang, JK, Malerba, A, Popplewell, L, Foster, K, Dickson, G (2011). Antisense-induced myostatin exon skipping leads to muscle hypertrophy in mice following octa-guanidine morpholino oligomer treatment. *Mol Ther* **19**: 159-164.
21. Kemaladewi, DU, Hoogaars, WM, van Heiningen, SH, Terlouw, S, de Gorter, DJ, den Dunnen, JT *et al*. (2011). Dual exon skipping in myostatin and dystrophin for Duchenne muscular dystrophy. *BMC Med Genomics* **4**: 36.
22. Wagner, KR, McPherron, AC, Winik, N, Lee, SJ (2002). Loss of myostatin attenuates severity of muscular dystrophy in mdx mice. *Ann Neurol* **52**: 832-836.
23. Krivickas, LS, Walsh, R, Amato, AA (2009). Single muscle fiber contractile properties in adults with muscular dystrophy treated with MYO-029. *Muscle Nerve* **39**: 3-9.
24. Wagner, KR, Fleckenstein, JL, Amato, AA, Barohn, RJ, Bushby, K, Escolar, DM *et al*. (2008). A phase I/IItrial of MYO-029 in adult subjects with muscular dystrophy. *Ann Neurol* **63**: 561-571.
25. Andreetta, F, Bernasconi, P, Baggi, F, Ferro, P, Oliva, L, Arnoldi, E *et al*. (2006). Immunomodulation of TGF-beta 1 in mdx mouse inhibits connective tissue proliferation in diaphragm but increases inflammatory response: implications for antifibrotic therapy. *J Neuroimmunol* **175**: 77-86.
26. Nelson, CA, Hunter, RB, Quigley, LA, Girgenrath, S, Weber, WD, McCullough, JA *et al*. (2011). Inhibiting TGF-beta Activity Improves Respiratory Function in mdx Mice. *Am J Pathol* **178**: 2611-2621.
27. Cohn, RD, van, EC, Habashi, JP, Soleimani, AA, Klein, EC, Lisi, MT *et al*. (2007). Angiotensin II type 1 receptor blockade attenuates TGF-beta-induced failure of muscle regeneration in multiple myopathic states. *Nat Med* **13**: 204-210.
28. Spurney, CF, Sali, A, Guerron, AD, Iantorno, M, Yu, Q, Gordish-Dressman, H *et al*. (2011). Losartan decreases cardiac muscle fibrosis and improves cardiac function in dystrophin-deficient mdx mice. *J Cardiovasc Pharmacol Ther* **16**: 87-95.
29. Souza, TA, Chen, X, Guo, Y, Sava, P, Zhang, J, Hill, JJ *et al*. (2008). Proteomic identification and functional validation of activins and bone morphogenetic protein 11 as candidate novel muscle mass regulators. *Mol Endocrinol* **22**: 2689-2702.
30. Dennler, S, Itoh, S, Vivien, D, ten, DP, Huet, S, Gauthier, JM (1998). Direct binding of Smad3 and Smad4 to critical TGF beta-inducible elements in the promoter of human plasminogen activator inhibitor-type 1 gene. *EMBO J* **17**: 3091-3100.
31. Kemaladewi, DU, de Gorter, DJ, Aartsma-Rus, A, van Ommen, GJ, ten Dijke, P, 't Hoen, PA *et al*. (2011). Cell-type specific regulation of myostatin signaling. *FASEB J*.
32. Wu, B, Li, Y, Morcos, PA, Doran, TJ, Lu, P, Lu, QL (2009). Octa-guanidine morpholino restores dystrophin expression in cardiac and skeletal muscles and ameliorates pathology in dystrophic mdx mice. *Mol Ther* **17**: 864-871.
33. Dumonceaux, J, Marie, S, Beley, C, Trollet, C, Vignaud, A, Ferry, A *et al*. (2010). Combination of myostatin pathway interference and dystrophin rescue enhances tetanic and specific force in dystrophic mdx mice. *Mol Ther* **18**: 881-887.
34. Stedman, HH, Sweeney, HL, Shrager, JB, Maguire, HC, Panettieri, RA, Petrof, B *et al*. (1991). The mdx mouse diaphragm reproduces the degenerative changes of Duchenne muscular dystrophy. *Nature* **352**: 536-539.
35. Liu, D, Black, BL, Derynck, R (2001). TGF-beta inhibits muscle differentiation through functional repression of myogenic transcription factors by Smad3. *Genes Dev* **15**: 2950-2966.
36. Moyer, AL and Wagner, KR (2011). Regeneration versus fibrosis in skeletal muscle. *Curr Opin Rheumatol* **23**: 568-573.
37. Amthor, H, Macharia, R, Navarrete, R, Schuelke, M, Brown, SC, Otto, A *et al*. (2007). Lack of myostatin results in excessive muscle growth but impaired force generation. *Proc Natl Acad Sci U S A* **104**: 1835-1840.
38. Pistilli, EE, Bogdanovich, S, Goncalves, MD, Ahima, RS, Lachey, J, Seehra, J *et al*. (2011). Targeting the activin type IIB receptor to improve muscle mass and function in the mdx mouse model of duchenne muscular dystrophy. *Am J Pathol* **178**: 1287-1297.
39. Kano, MR, Komuta, Y, Iwata, C, Oka, M, Shirai, YT, Morishita, Y *et al*. (2009). Comparison of the effects of the kinase inhibitors imatinib, sorafenib, and transforming growth factor-beta receptor inhibitor on extravasation of nanoparticles from neovasculature. *Cancer Sci* **100**: 173-180.
40. Sugiyama, M, Ichida, T, Sato, T, Ishikawa, T, Matsuda, Y, Asakura, H (1998). Expression of activin A is increased in cirrhotic and fibrotic rat livers. *Gastroenterology* **114**: 550-558.
41. Patella, S, Phillips, DJ, Tchongue, J, de Kretser, DM, Sievert, W (2006). Follistatin attenuates early liver fibrosis: effects on hepatic stellate cell activation and hepatocyte apoptosis. *Am J Physiol Gastrointest Liver Physiol* **290**: G137-G144.

42. Kalluri, R and Neilson, EG (2003). Epithelial-mesenchymal transition and its implications for fibrosis. *J Clin Invest* **112**: 1776-1784.

43. Ruijter, JM, Ramakers, C, Hoogaars, WM, Karlen, Y, Bakker, O, van den Hoff, MJ *et al*. (2009). Amplification efficiency: linking baseline and bias in the analysis of quantitative PCR data. *Nucleic Acids Res* **37**: e45.

44. van Putten, M, de, WC, van Roon-Mom, W, van Ommen, GJ, 't Hoen, PA, Aartsma-Rus, A (2010). A 3 months mild functional test regime does not affect disease parameters in young mdx mice. *Neuromuscul Disord* **20**: 273-280.

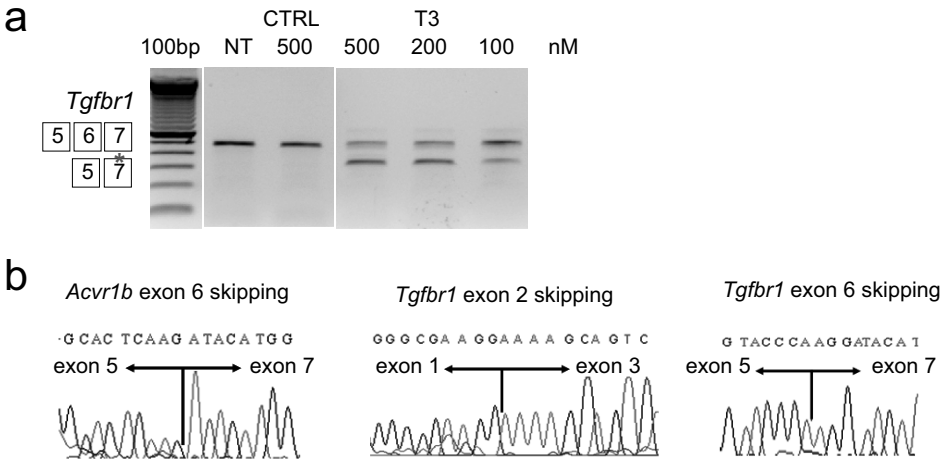


**Supplementary figure 1. *Tgfbr1* exon 6 skipping *in vitro* and sequence analysis of successful exon skipping in this study.** RT-PCR analysis of C2C12 myoblasts transfected with CTRL or increasing concentration of T3 AON, which target exon 6 of *Tgfbr1* (**a**) show the desired products. This AON was ineffective *in vivo* and therefore omitted from this study. Sequence analysis was performed to confirm the identity of the skipped products (**b**).

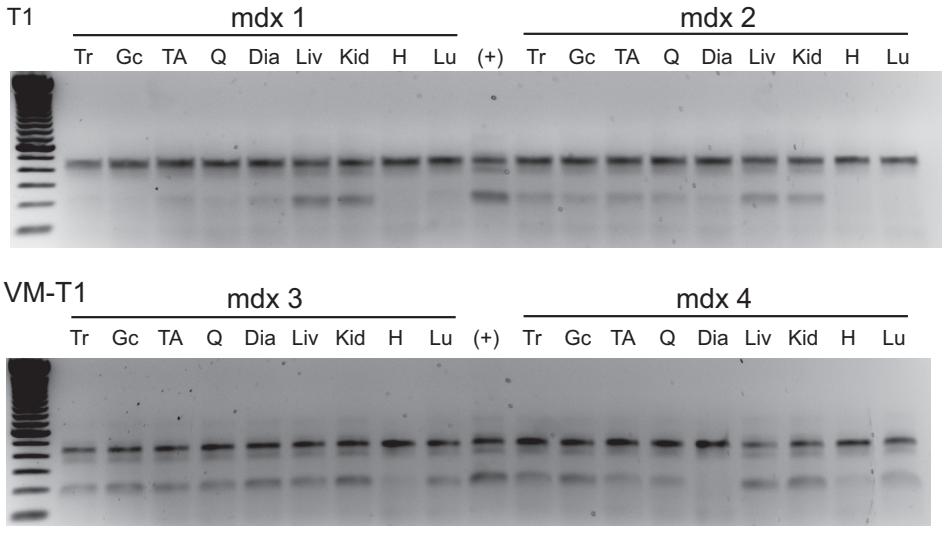


**Supplementary figure 2. Comparison of *Tgfbr1* exon 2 skipping levels in different tissues after systemic administration of different AON chemistries.** *mdx* mice were treated with 2 times 100 mg/kg of T1, which consists of 2'-O-Methyl phosphorothioate modifications (upper panel) or 2 times 6mg/kg VM-T1, which consists of phosphorodiamidate morpholino oligomers linked to an oligodendrimer group (lower panel), both targeting exon 2 of *Tgfbr1*. The injections were performed daily for 2 days via intravenous route. All animals were sacrificed 4 days after the last injection and different tissues were collected. Tr = Triceps, Gc = Gastrocnemius, TA = Tibialis anterior, Q = quadriceps, Dia = Diaphragm, Liv = Liver, Kid = Kidney, H = Heart, Lu = Lung, (+) = positive control.

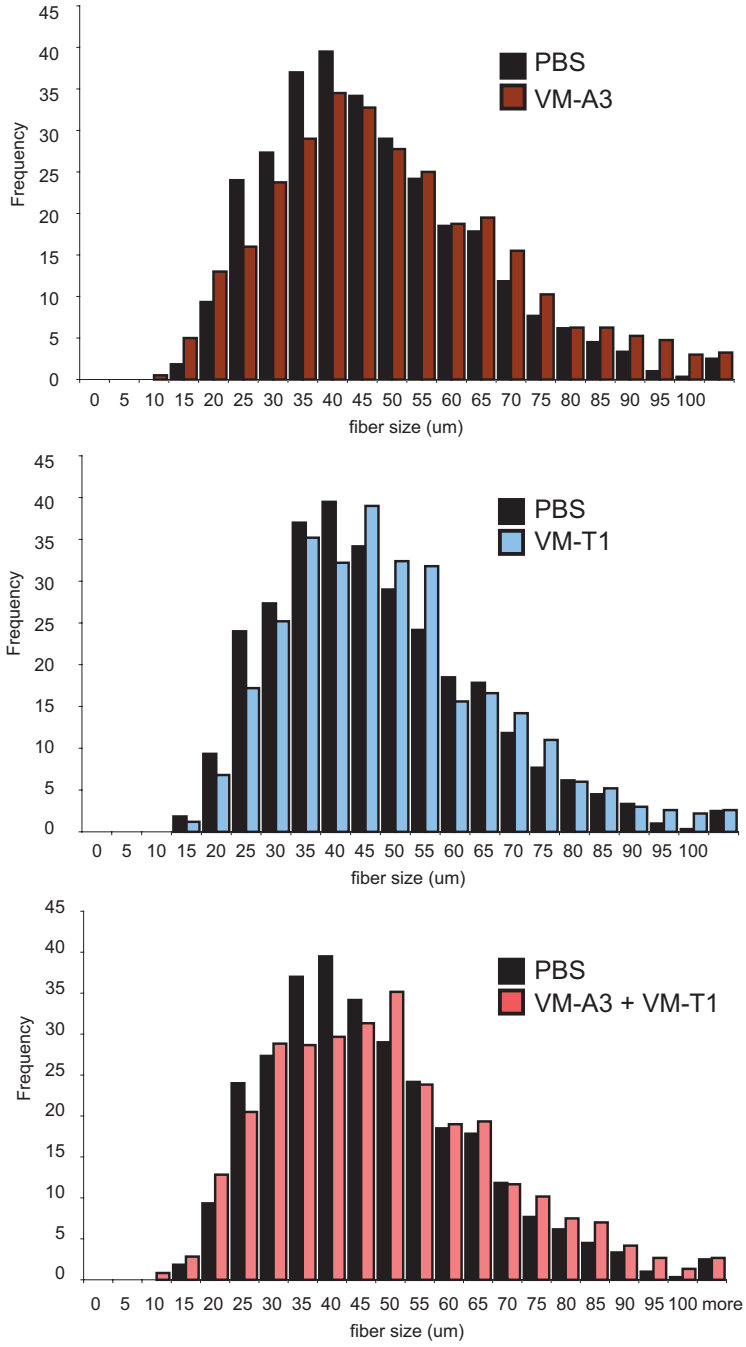


**Supplementary figure 3. Triceps myofiber diameter following systemic administration.** Distribution of triceps fiber diameters in PBS (black bars) compared to VM-A3- (brown), VM-T1- (blue) and combination of VM-A3+VM-T1 (pink) treated animals. 300 fibers were counted per animals and the average for 6 animals per group was plotted.

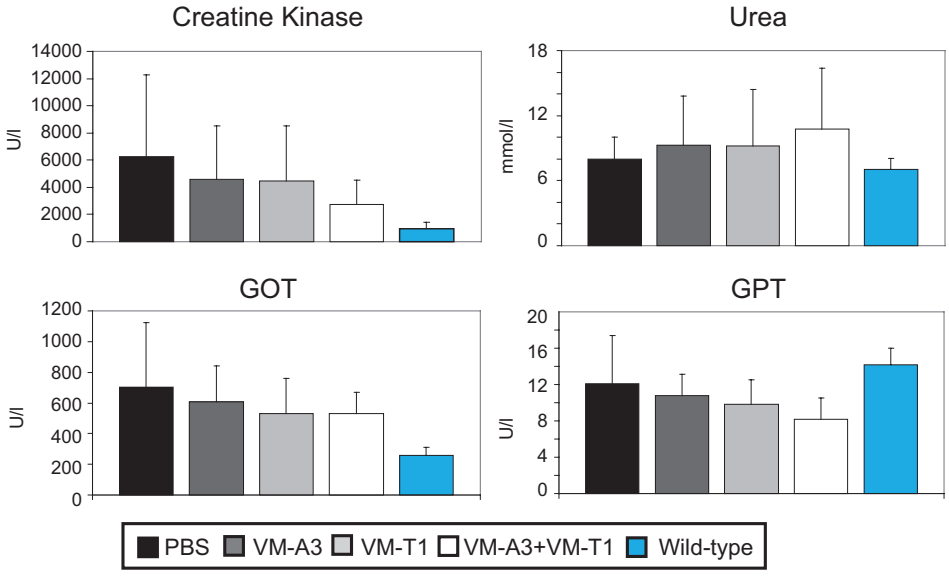


**Supplementary figure 4. Serum protein analysis at the end point of systemic administration.** Blood was taken from tails for each animal at the terminal time point and serum was collected. Urea, glutamic-pyruvic transaminase (GPT), glutamic-oxaloacetic transaminase (GOT) and Creatine kinase (CK) levels were measured. The average values of all animals in each group was calculated and plotted. Error bars represent the standard deviation.